

Article

Energy-Exergy–Economic (3E) -Optimization Analysis of a Solar System for Cooling, Heating, Power, and Freshwater Generation System for a Case Study Using Artificial Intelligence (AI)

Mohammad Reza Assari ^{1,2,†}, Ehsanolah Assareh ^{3,4,*}, Neha Agarwal ^{4,†}, Milad Setareh ¹, Nazanin Alaei ^{1,†}, Ali Moradian ¹ and Moonyong Lee ^{4,*} 

¹ Mechanical Engineering Department, Jundi-Shapur University of Technology, Dezful 64615-334, Iran; msetare@jsu.ac.ir (M.S.)

² Department of Mechanical Engineering, Faculty of Engineering, Alzahra University, Tehran 19938-93973, Iran

³ Department of Mechanical Engineering, Dezful Branch, Islamic Azad University, Dezful 313, Iran

⁴ School of Chemical Engineering, Yeungnam University, Gyeongsan 38541, Republic of Korea

* Correspondence: ehsanolah.assareh@yu.ac.kr (E.A.); mynlee@yu.ac.kr (M.L.)

† These authors contributed equally to this work.

Abstract: In this research, analysis of a cogeneration system harnessing solar energy with the purpose of producing electricity and freshwater is carried out. A parabolic trough collector (PTC), a reverse osmosis (RO) desalination system and a steam Rankine cycle are considered as the primary modules of the system. Optimization is conducted on the basis of the Non-Dominated Sorting Genetic Algorithm II (NSGA-II), while the Engineering Equation Solver (EES) is used to cope with the presented thermodynamic model. Sensitivity analysis of different key parameters including pump and turbine efficiencies, pump and turbine inlet pressures, evaporator pinch point and inlet temperature and, finally, solar radiation are calculated. A location with high solar energy potential is selected to explore the feasibility of installing the designed system. The case study results show that the maximum level of freshwater production happens during June and July due to an increased sunlight and ambient temperature. Annual electricity and distilled water production of 260,847.6586 MW and 73,821.34 m³ are calculated, respectively. Furthermore, the optimum results regarding the cost rate and exergy efficiency were found to be 35.26 \$/h and 12.02%, respectively.

Keywords: solar energy; parabolic trough solar collector; exergy efficiency; cost rate



Citation: Assari, M.R.; Assareh, E.; Agarwal, N.; Setareh, M.; Alaei, N.; Moradian, A.; Lee, M.

Energy-Exergy–Economic (3E) -Optimization Analysis of a Solar System for Cooling, Heating, Power, and Freshwater Generation System for a Case Study Using Artificial Intelligence (AI). *Energies* **2023**, *16*, 4873. <https://doi.org/10.3390/en16134873>

Academic Editors: Bartłomiej Iglński and Abu-Siada Ahmed

Received: 10 March 2023

Revised: 13 June 2023

Accepted: 16 June 2023

Published: 22 June 2023



Copyright: © 2023 by the authors. Licensee MDPI, Basel, Switzerland. This article is an open access article distributed under the terms and conditions of the Creative Commons Attribution (CC BY) license (<https://creativecommons.org/licenses/by/4.0/>).

1. Introduction

In recent years, scientists have strived to build and develop alternative technologies to respond to the energy demands as well as energy crises. In addition to increasing security and independence at the national level, solar energy reduces the environmental pollution and has a significant impact on the conservation of environmental resources and also fossil deposits. In a 2021 research study [1], the uses of different solar thermal collectors to satisfy the electrical requirements of a power plant are compared. The utilization of the sun's power is performed as a way to heat up the feed water of the boiler and, as a result, reduce fuel consumption and exergy destruction of the power plant. A parabolic solar collector and a linear one were studied and their performance was evaluated. The results of exergy analysis for the two types of solar collectors showed that the parabolic trough collector (PTC) outperforms the other one. Kumargupta et al. [2] designed a proposed system including an organic Rankine cycle with a triple pressure level absorption system and a PTC. This system produces electric energy and cooling at two different temperatures simultaneously. The results showed that when the ambient temperature increases from 5 °C to 35 °C, the energy production is reduced to 6.8 MW. In addition, exergy efficiency decreased from 54.9% to 36.7% while representing an increase in the cost. Alirahmi et al. [3]

discussed a new energy system, which functions by harnessing solar and geothermal energy to produce electricity, heating, cooling, hydrogen and freshwater. The results showed that the exergy efficiency of the system and the total cost of the unit reach 29.95% and 129.7 GJ/h, respectively, at the optimal level. Keshavarzadeh and Ahmadi [4] worked on the multi-objective optimization of a solar energy system. In their study, they used various optimization techniques. Multi-objective optimization was used to investigate the two objective functions of exergy efficiency and total cost rate. They used techniques such as MPMO, IBEA, SPEA and NSGA-II for optimization. Qureshi et al. [5] worked on the energy and exergy analyses of a cogeneration system based on solar renewable energy for electricity and hydrogen production. The results showed that the proposed system has 25.07% energy efficiency and 31.01% exergy efficiency. The highest efficiency of energy and exergy for 1000 MW of input heat from the solar receiver was obtained, equal to 33.53% and 41.49%, respectively. Behzadi et al. [6] performed a multi-objective design optimization of a solar-based system for electricity and hydrogen production. The optimization of this research was performed by a genetic algorithm. In their research, a thermoelectric generator was used instead of a condenser to increase exergy efficiency and electricity production, increase the amount of hydrogen production and reduce the cost rate. The results of the study showed that the proposed thermoelectric system has higher exergy efficiency, higher hydrogen production rate and a lower total cost rate. Yuksel et al. [7] investigated the thermodynamic assessment of a modified organic Rankine cycle (ORC) and parabolic trough collector (PTC) for hydrogen production. In their research, solar energy is converted into heat energy by using a parabolic collector, and then the heat energy produced in the modified ORC is used to generate electricity. Then the electricity is used to produce hydrogen. It was possible to produce hydrogen, cooling and electricity. Gholaminian et al. [8] studied the multi-objective optimization of a geothermal-based organic Rankine cycle with a thermoelectric generator that was used to produce electric energy and hydrogen. The thermal energy of the organic processed fluid was absorbed from the brine of geothermal water passed between the evaporator and the superheater. The working fluid of the organic cycle after passing through the salt water turbine and producing power is returned to the evaporator before being pumped. [8]. Haideranjad et al. [9] presented an extensive method for enhancing a biomass-assisted geothermal power plant with freshwater generation. The combustion of urban solid waste was utilized to improve the performance of the system, and the exhaust gases of urban solid waste combustion were used as the main source of energy for the multi-purpose desalination subsystem. The results showed that the energy and exergy efficiency of the system can reach 13.9% and 19.4%, respectively, while the cost rate of the entire system was estimated at 285.3 \$/h. Ghorbani et al. [10] used a water treatment supplier, water heater and parabolic trough solar collector in water and electric energy production factories. To provide input heat, the structure of parabolic trough solar collectors was used, and to supply the cooling system of the organic Rankine cycle condenser, a degassing operation was used again. This energy production system is capable of producing 3628 kg/h of freshwater and 459.9 MW of electric power. Kian Fard et al. [11] worked on the exergy and exergoeconomic evaluation of hydrogen and distilled water production based on geothermal energy and using two organic Rankine cycles, reverse osmosis or desalination system, and an electrolyzer. The total investment costs for the reverse osmosis water treatment supplier unit were found to be 56% with economic analysis. The cost rate of freshwater production was calculated to be 32.73 cents/m³. Alirahmi and Asareh [12] investigated and analyzed the energy, exergy and exergoeconomics and multi-objective optimization of a multi-generation energy system including production of hydrogen, freshwater, cooling, heating and hot water as well as electricity production in Dezful, Iran. Two objective functions of this research, exergy and total cost, were introduced, which were optimized with the genetic algorithm. In the Pareto frontier, the best point was selected with the TOPSIS decision criterion, which obtained the best value for the exergy efficiency of 31.66% and the total unit rate of 21.9 GJ/\$. Assareh et al. [13] worked on a renewable system based on the use of solar and geothermal energy boosted

with thermoelectric generators (TEG) for electricity, cooling and desalination production. In this system, instead of a condenser, thermoelectric generators were used to increase the electricity produced by SRC. The results showed that the use of TEG instead of the condenser led to a decrease in the total cost rate and an increase in the exergy efficiency of the system. Razmi et al. [14] investigated an efficient and environmentally friendly power generation system based on compressed air storage, an organic Rankine cycle and a vapor compression refrigeration cycle. The results showed that the overall exergy efficiency and exergy destruction of the components were 49.17% and 1419 kW, respectively, where the pressure regulating valve and air turbine have the highest irreversibility and exergy loss.

The purpose of this research is to model and optimize a cogeneration system by harnessing solar power and using a PTC to feed more solar energy and improve the system's performance. A thermodynamic model of the system is presented. Further, the governing equations are solved by the Engineering Equation Solver (EES). Then, the parametric study for investigating the impact of different parameters is carried out. Afterwards, the system is optimized using the multi-objective algorithm (NSGA-II) to determine the optimum points.

2. Methodology

2.1. Energy System

The schematic of the proposed solar system is showed in Figure 1. It consists of a parabolic trough solar collector, steam Rankine cycle and reverse osmosis desalination system. It is worthy to notice that the length and width of PTCs have a direct impact on the amount of heat transfer. The heat transfer produced from the collector is applied according to the characteristics of the solar system. The task of the parabolic solar collector is to convert solar radiant energy into thermal energy. The parabolic solar collector absorbs the radiant energy of the sun and then transfers significant heat to the working fluid of the collector. This energy is then directed to the steam Rankine cycle for utilization. The steam Rankine cycle is used to generate electricity and consists of four pieces of equipment: an evaporator, a turbine, a condenser and a pump. In this research, after achieving the temperature of 300 °C at point 1, the working fluid enters the Rankine cycle, and at point 4, it enters the turbine and causes it to rotate, which produces electricity. It is necessary to mention that the saturated steam with a quality of 1 leaves the evaporator and goes to the Rankine cycle steam turbine and produces electricity. At point 5, a water fluid with lower pressure and temperature enters the condenser and then enters the pump, and this cycle is repeated again. At points 12 and 13, a reverse osmosis desalination system is used. Desalination of seawater is one of the important issues and parameters; as a result, seawater enters the reverse osmosis desalination unit and finally freshwater is supplied. The electricity required by the reverse osmosis desalination unit is provided by the electricity produced by the system, and this is one of the advantages of the proposed system. The reverse osmosis unit is responsible for purifying water and separating salts from salty seawater. In this system, the pressure is used to reverse the osmotic flow of water through a semi-permeable membrane to produce pure water and remove ions, molecules and larger particles dissolved in the water.

2.2. Thermodynamic Modeling and Evaluation

A balance of mass and energy should be considered for every control volume. Therefore, the assumptions and constraints in our study are as follows:

1. A steady state setting;
2. An isentropic condition is considered for both pumps and turbines;
3. The pressure drop in pipelines is insignificant [15];
4. The outlet of the condenser is saturated liquid and the outlet of the evaporator is saturated vapor [15];
5. Variations of kinetic and potential energy are insignificant [16].

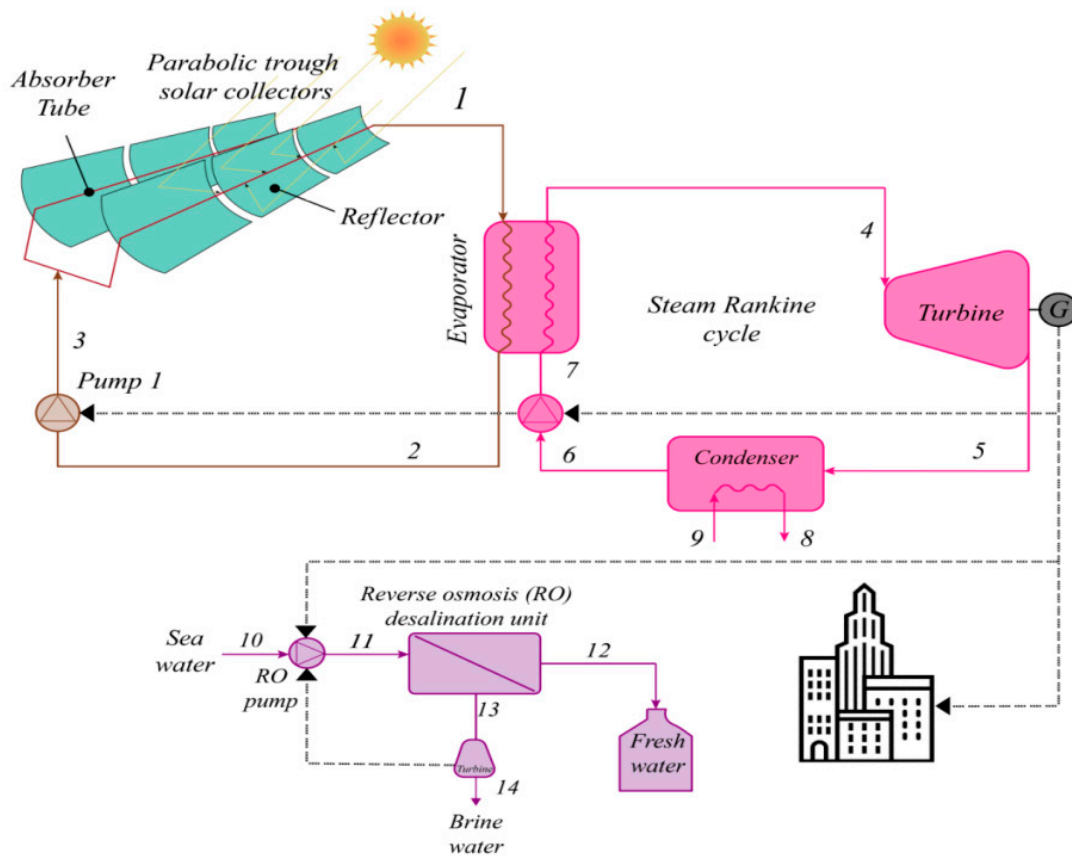


Figure 1. Schematic of the proposed system.

Table 1 shows all input and operating parameters regarding the thermodynamic analysis.

Table 1. Input data [3,12,13].

No.	Parameter	Symbol	Value
1	Ambient temperature	T_0	25 [°C]
2	Pressure	P_0	101.3 [kPa]
3	Sun temperature	T_{sun}	5800 [°C]
4	Input temperature to evaporator	T_1	300 [°C]
5	Inlet flow rate to evaporator	\dot{m}_1	10 [kg/h]
6	Solar radiation intensity	G_b	850 [W/m ²]
7	Transmissivity of collector cover	τ	0.96 [-]
8	Turbine efficiency	$\eta_{turbine}$	0.85 [-]
9	Pump efficiency	η_{pump}	0.9 [-]
10	Evaporator pinch point	pp_{Eva}	5 [°C]
11	Condenser pinch point	pp_{Cond}	5 [°C]
12	Input pressure to turbine	P_4	1500 [Kpa]
13	Input pressure to pump	P_6	100 [Kpa]
14	Input pressure to evaporator	P_1	250 [Kpa]
15	Heat loss collector coefficient	U_l	3.82 [W/m ² .°C]

The general form of the first rule of thermodynamics is given according to the following equation. Table 2 shows the energy balance equation for each part, which is derived by using the first law of thermodynamics.

$$\dot{Q} - \dot{W} + \sum_i \dot{m}_i \left(h_i + \frac{v_i^2}{2} + gZ_i \right) - \sum_e \dot{m}_e \left(h_e + \frac{v_e^2}{2} + gZ_e \right) = \frac{dE_{cv}}{dt} \quad (1)$$

Table 2. Energy balance.

System Components	Energy Balance
Turbine	$\dot{W}_{turbine} = \dot{m}_4 \times (h_4 - h_5)$
Condenser	$Q_{cond} = \dot{m}_5 \times (h_5 - h_6)$
Evaporator	$Q_{Eva} = \dot{m}_7 \times (h_4 - h_7)$
Pump No. 1	$\dot{W}_{pump1} = \dot{m}_2 \times (h_3 - h_2)$
Pump No. 2	$\dot{W}_{pump2} = \dot{m}_6 \times (h_7 - h_6)$
Solar collector	$Q_{sc} = \dot{m}_3 \times (h_1 - h_3)$

Equation (2) is used to calculate the net energy of the system:

$$\dot{W}_{net} = \dot{W}_{turbine} - \dot{W}_{pump1} - \dot{W}_{pump2} \quad (2)$$

2.3. Parabolic Solar Collector Analysis

Using the following equations, the amount of useful energy produced in the PTC is obtained by both Equations (3) and (4) as follows [7,17,18]:

$$\dot{Q}_u = \dot{m}_1 [C_{p,c} \times T_1 - C_{p,c} \times T_3] \quad (3)$$

$$\dot{Q}_u = n_{ptc} F_R [S A_{ap} - A_r U_L (T_3 - T_0)] \quad (4)$$

S is estimated according to Equation (5) [13]:

$$S = G_b \tau_C \tau_P \alpha \quad (5)$$

In addition, F_1 and F_R parameters are specified by the following equations [7,18]:

$$F_R = \frac{\dot{m}_c C_{p,c}}{A_r U_L} \left[1 - \exp \left(- \frac{A_r U_L F_1}{\dot{m}_c C_{p,c}} \right) \right] \quad (6)$$

$$F_1 = \frac{\frac{1}{U_L}}{\frac{1}{U_L} + \frac{D_{o,r}}{h_{fi}} + \left(\frac{D_{o,r}}{2k} \ln \frac{D_{o,r}}{D_{i,r}} \right)} \quad (7)$$

2.4. Reverse Osmosis Analysis (RO)

The output power of the reverse osmosis pump is calculated from the following equation [19–21]:

$$P_{outputPower} = \dot{W}_{turbine} \times 0.3 \quad (8)$$

The fresh water rate can be estimated as follows:

$$Fresh\ Water\ Rate = (p_1 \times PumpPower^2 + p_2 \times PumpPower + p_3) / (PumpPower + q_1) \quad (9)$$

$$Fresh\ Water\ Rate = \dot{m}_{11} \quad (10)$$

Table 3 shows the coefficients of Equation (9) for calculating the freshwater rate:

Table 3. Coefficients of freshwater rate equation [12,13].

Coefficients	Value
p_1	0.06739 (-)
p_2	183.2 (-)
p_3	130.2 (-)
q_1	867.3 (-)

2.5. Exergy Analysis

In order to perform the exergy analysis, Equations (11)–(14) are considered:

$$\dot{E}x_Q + \sum_{in} \dot{m}_{in} ex_{in} = \dot{E}x_W + \dot{E}x_D + \sum_{out} \dot{m}_{out} ex_{out} \quad (11)$$

Here,

$$\dot{E}x_W = \dot{W} \quad (12)$$

$$\dot{E}x_Q = Q_j \left(1 - \frac{T_0}{T_j} \right) \quad (13)$$

$$ex = ex_{ph} + ex_{ch} \quad (14)$$

2.6. Economic Evaluation

Equation (15) refers to the capital recovery factor (CRF) [22]:

$$CRF = \frac{i(1+i)^n}{(1+i)^n - 1} \quad (15)$$

where i is assumed to be 0.1 and n is 20.

Equation (16) expresses the cost rate for each part [22]:

$$\dot{Z}_k = \frac{Z_k CRF \varphi}{N} \quad (16)$$

where φ is indicative of the maintenance factor for the system and its value is equal to 1.06. In this regard, N is the number of working hours of the system. In Table 4, the equations related to the cost calculation of the desired system components are written.

Table 4. Cost balance and auxiliary equations for all system components [3,13,14].

Equation No.	Component	Equation
17	Turbine	$Z_{Tur} = 4750 \left(\dot{W}_{turbine}^{0.75} \right) + 60 \left(\dot{W}_{turbine}^{0.95} \right)$
18	Condenser	$Z_{Cond} = 1773 \times \dot{m}_5$
19	Evaporator	$Z_{Eva} = 276 (A_{Eva}^{0.88})$
20	Pump No. 1	$Z_{Pump1} = 3500 \left(\dot{W}_{Pump1}^{0.41} \right)$
21	Pump No. 2	$Z_{Pump2} = 3500 \left(\dot{W}_{Pump2}^{0.41} \right)$
22	Solar collector	$Z_{PTC} = 240 A_P$
23	Reverse osmosis	$Z_{RO} = 0.98 \dot{m}_{12}$

3. Results and Discussion

3.1. Validation

Due to the fact that the designed system is a new system and has not been investigated before, there is not much data for a verification. In order to validate and check the correctness of the written code, a comparison of the current study and the results of Ref. [23] has been performed and is presented in Table 5. As the results show, the modeling has a proper validity.

Table 5. Comparison between results by present code and by Nafey and Sharaf [23].

Parameter	Unit	Current Research	Nafey and Sharaf [23]	Difference (%)
$W_{pump, RO}$	kW	1122	1131	0.796
M_f	m ³ /h	485.9	485.9	0
SR	-	0.9944	0.9944	0
X_b	ppm	64,180	64,180	0
X_d	ppm	252	250	0.8
ΔP	kPa	6856	6850	0.088

3.2. Sensitivity Analysis

Sensitivity analysis has the ability to consider every studied parameter and probable result, thus assisting crucial decisions. Table 6 shows a range of design parameters for sensitivity analysis and parametric study of the system. This range has been selected for the system's analysis according to the investigations carried out in previous studies.

Table 6. Range of the design parameters.

Design Parameters	Upper Limit	Lower Limit
Efficiency of pump (%)	0.95	0.75
Efficiency of turbine (%)	0.95	0.75
Turbine inlet pressure (kPa)	1600	1400
Pump inlet pressure (kPa)	110	90
Evaporator pinch point (°C)	5	15
Solar radiation (W/m ²)	400	900
Evaporator inlet temperature (°C)	400	300

In order to calculate the results of this stage, the amount of growth or decrease in changes of production power, fresh water production rate, exergy efficiency and cost rate are compared to the rise in the design parameters introduced in Table 7. In this table, the highest and the lowest values of each output were obtained, and then the growth or decrease in percentage of each output was calculated.

Table 7. Sensitivity analysis.

No.	Parameter	Total Work (kW)	Rate of Fresh Water (m ³ /h)	Exergy Efficiency (%)	Cost Rate (\$/h)
1	Efficiency of pump	Max: 606.9 Min: 606.3 Difference = 0.09%	Max: 34.04 Min: 34.01 Difference = 0.08%	Max: 12.31 Min: 12.3 Difference = 0.08%	Max: 35.44 Min: 35.43 Difference = 0.02%
2	Efficiency of turbine	Max: 678.5 Min: 535.1 Difference = 26.72%	Max: 37.55 Min: 30.43 Difference = 23.39%	Max: 13.76 Min: 10.85 Difference = 26.82%	Max: 36.33 Min: 34.51 Difference = 5.27%
3	Turbine inlet pressure	Max: 620.1 Min: 592.5 Difference = 4.65%	Max: 34.69 Min: 33.32 Difference = 4.11%	Max: 12.58 Min: 12.02 Difference = 4.65%	Max: 35.6 Min: 35.24 Difference = 1.02%
4	Pump inlet pressure	Max: 623.2 Min: 591.6 Difference = 5.41%	Max: 34.85 Min: 33.28 Difference = 4.71%	Max: 12.64 Min: 12 Difference = 5.33%	Max: 35.64 Min: 35.24 Difference = 1.13%
5	Evaporator pinch point	Max: 608.3 Min: 606.8 Difference = 0.24%	Max: 34.11 Min: 34.03 Difference = 0.23%	Max: 12.34 Min: 12.31 Difference = 0.25%	Max: 35.45 Min: 35.43 Difference = 0.05%
6	Solar radiation	Max: 643.1 Min: 497.8 Difference = 29.37%	Max: 35.83 Min: 28.52 Difference = 25.63%	Max: 12.32 Min: 12.26 Difference = 0.48%	Max: 35.9 Min: 33.98 Difference = 5.65%
7	Evaporator inlet temperature	Max: 360 Min: 340 Difference = 5.88%	Max: 34.26 Min: 34.03 Difference = 0.67%	Max: 12.4 Min: 12.31 Difference = 0.73%	Max: 35.5 Min: 35.43 Difference = 0.19%

It can be concluded from Table 7 that, in the present research, the most influential decision variables having effects on the performance of the system are the turbine input pressure and turbine efficiency. The reasons for such changes in the system outputs compared to the growth or decrease of the design parameters can be stated as follows:

- Power production and exergy efficiency are directly related to each other, so by increasing or decreasing the power production of the system, the value of exergy efficiency increases or decreases as well.
- With the increase in the production capacity of the system and the need for larger equipment and more maintenance, the cost rate of the system also increases.
- The performance and efficiency of solar collectors depend more on the intensity of solar radiation than any other factor because all the power required to produce energy is provided by solar collectors from sunlight, and the higher the amount of solar radiation, the more efficient the solar collectors will be. It is also found that increasing or decreasing the performance of the solar collector has a direct effect on the performance of the system because the energy required by the Rankine cycle is provided by solar energy.
- With the increase in solar radiation, the flow rate of the input fluid to the solar collectors increases, and as a result, the output work of the subsystems also increases. With the increase in the flow rate, the total output work will also increase and vice versa.
- With the increase in the temperature of the evaporator, the input enthalpy to the steam Rankine cycle turbine also increases, and as a result, the total work increases with the increase in enthalpy and vice versa.
- As the pinch point temperature of the evaporator increases, its amount of heat transfer decreases; as a result, with the decrease in heat transfer from the evaporator to the steam Rankine cycle, the work output of the entire system does not increase much.
- Increasing or decreasing the amount of heat transfer has a direct relationship with the work of the whole system.
- By increasing the input pressure of the steam Rankine cycle turbine, the enthalpy of the fluid also increases at this point, and as a result, it increases the total work of the turbine and steam Rankine cycle, which increases the total work for this cycle.
- By increasing the input pressure of the steam Rankine cycle turbine, the output pressure from the turbine rises as well. The output pressure from the turbine increases the input energy to produce the power of the system, so with the increase in the input pressure of the turbine, the energy production also increases.

3.3. Parametric Study

A primary challenge of designing sustainable energy systems is to determine the optimum point of techno-economic viability and also to find out about different variables having impacts on the energy system.

In Figure 2 examines the impact of increasing turbine efficiency on the system's performance. Turbine efficiency means the ratio of practical power to total power. According to Figure 2, due to the increase in the efficiency of the turbine, the work output of the entire system and the rate of freshwater produced by the system increases, and considering that the output work and exergy efficiency are directly related to each other, we see an increase in the exergy efficiency of the system. Moreover, due to the increase in turbine efficiency, the cost rate of the system has also increased. The cause of such an increase in the cost rate lies in the rise in the work of the entire system, and a requirement for more equipment leads to increasing the system's costs.

In Figure 3, the effect of increasing the intensity of solar radiation on the performance of the system is investigated. The energy radiated from the surface of the sun is spread in the form of light and heat. The intensity of the sun's radiation increases and decreases with the sunrise and sunset, but it should be noted that its main changes are greater when the distance of the earth from the sun changes. Solar radiation determines the energy production performance of a solar system. The performance and efficiency of solar

collectors depend more on the intensity of solar radiation than any other factor because all the power required to produce energy is provided by solar collectors from sunlight, and the higher the amount of solar radiation, the more efficient the solar collectors will be. From Figure 3, it is evident that due to the increase in the intensity of the sun's radiation, the work rate of the whole system and the rate of freshwater produced by the system increase. It should be noted that the sun's radiation on the energy storage plate in renewable systems is one of the factors that has a very considerable effect on the performance of systems that use solar collectors. In other words, with the increase in solar radiation, the flow rate of the fluid entering the solar collectors increases, and as a result, the output work of the subsystems also increases. With the increase in the flow rate, the total output work will also increase, and vice versa. Moreover, we see an increase in the cost rate and exergy efficiency. With the increase in production capacity, the costs of system repairs and maintenance increase.

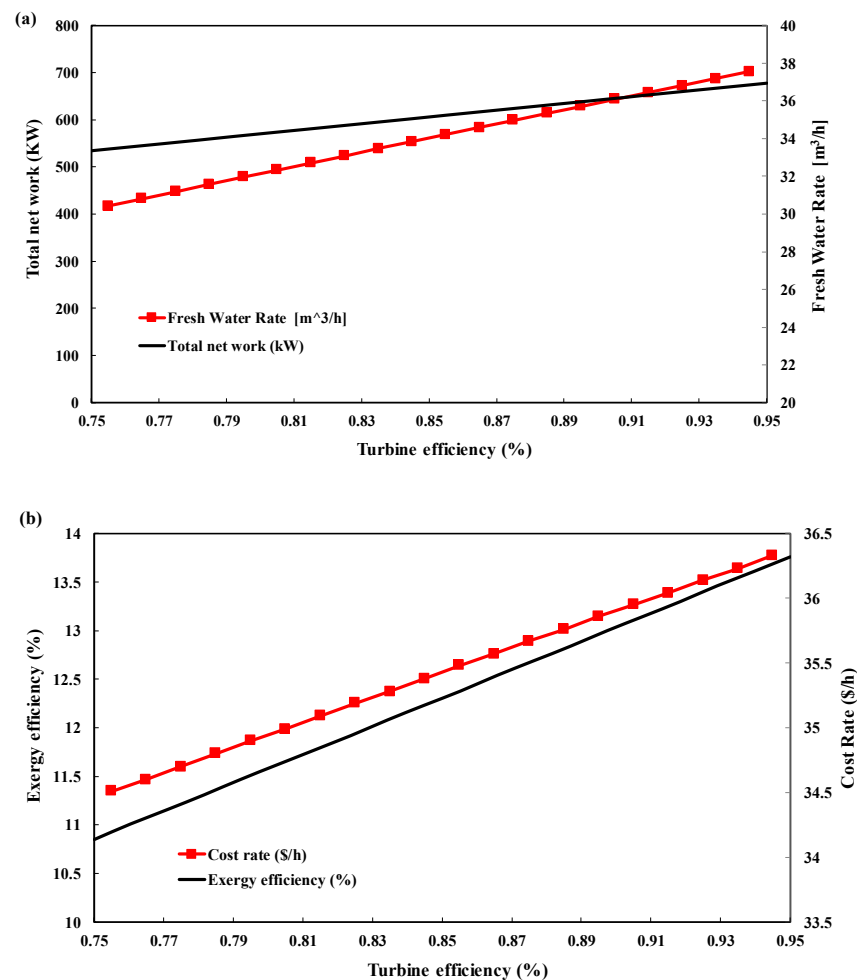


Figure 2. The effect of turbine efficiency on system outputs. (a) Work and fresh water (b) Exergy efficiency and cost rate.

Figure 4 examines the effect of increasing the input pressure of the turbine from 1400 kPa to 1600 kPa on the system outputs, which include the total work, rate of desalination production, exergy efficiency and cost rate. It can be seen that due to the increase in the input pressure of the turbine, the work rate of the entire system and the rate of freshwater produced by the system increases. Clearly, the exergy efficiency and system cost rate are also increasing due to an improvement in the system's performance and the increase in hidden and apparent costs of the system. Additionally, with the rise in the input pressure of the steam Rankine cycle turbine, the output pressure of the turbine also increases. The rise in the output pressure from the turbine increases the input energy to produce the power of

the system, so with the increase in the input pressure of the turbine, the output power also increases. As a result, the exergy efficiency of the system also increases due to the increase in total output power, and of course, the cost of the system also increases with the increase in production power.

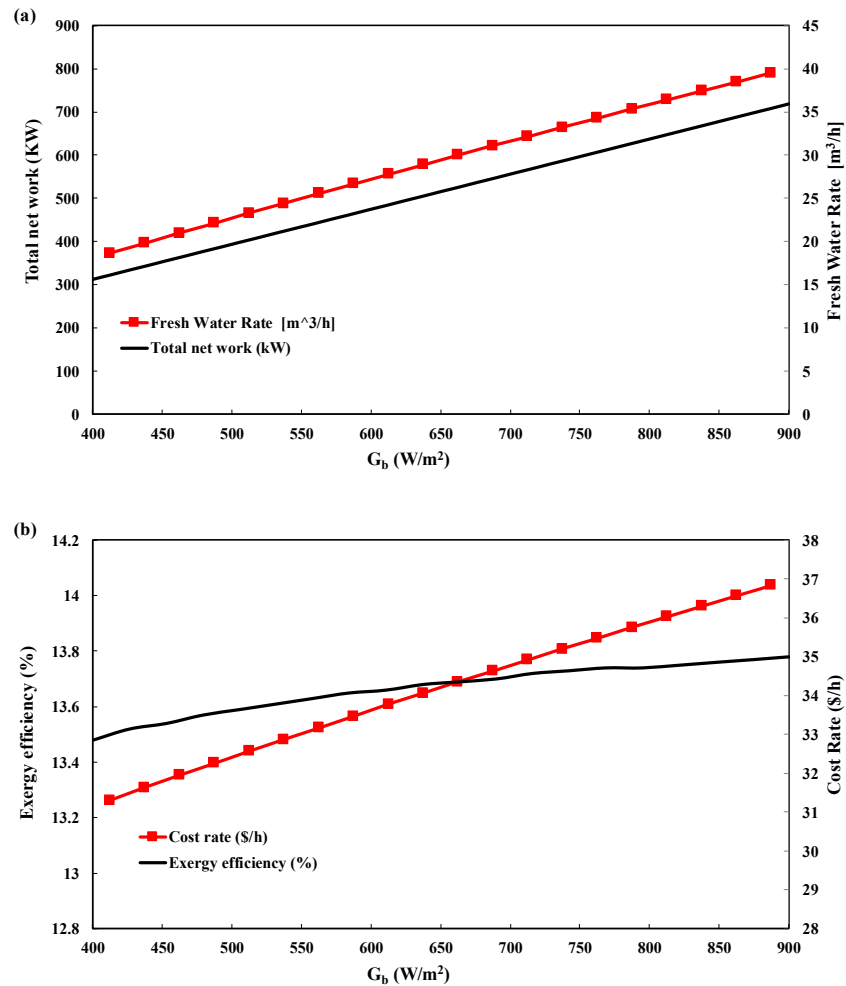


Figure 3. The effect of solar radiation on system outputs. (a) Work and fresh water (b) Exergy efficiency and cost rate.

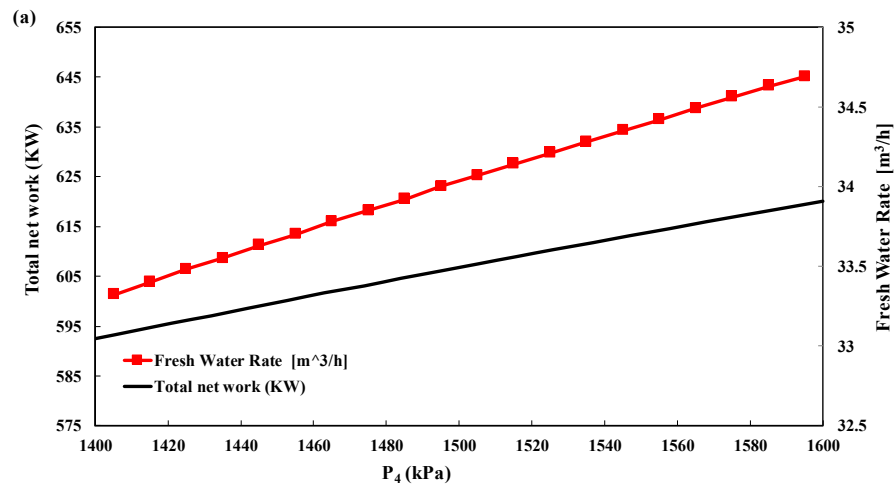


Figure 4. Cont.

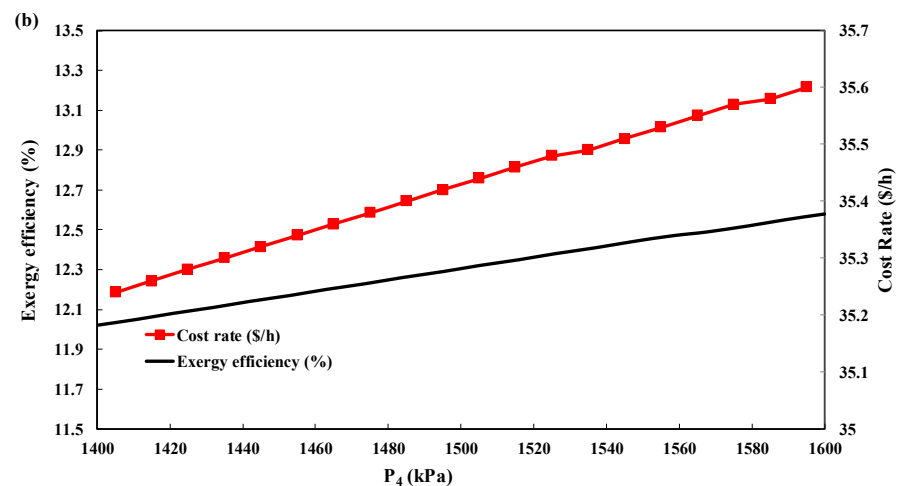


Figure 4. The effect of the turbine input pressure on the system outputs. (a) Work and fresh water (b) Exergy efficiency and cost rate.

4. Case Study

Due to the suitable location of Abadan, a southern city of Iran, in terms of suitable solar potential and high radiation of solar energy, and due to the existence of suitable conditions for this research, this city was chosen for the study. Next, for the city of Abadan, the hourly changes in air temperature and solar radiation throughout the year are shown in Figure 5. The information about Abadan city is extracted from Metanorm software 7.3. As shown, in the summer season, we see the highest temperature and the highest strength of solar radiation in Abadan.

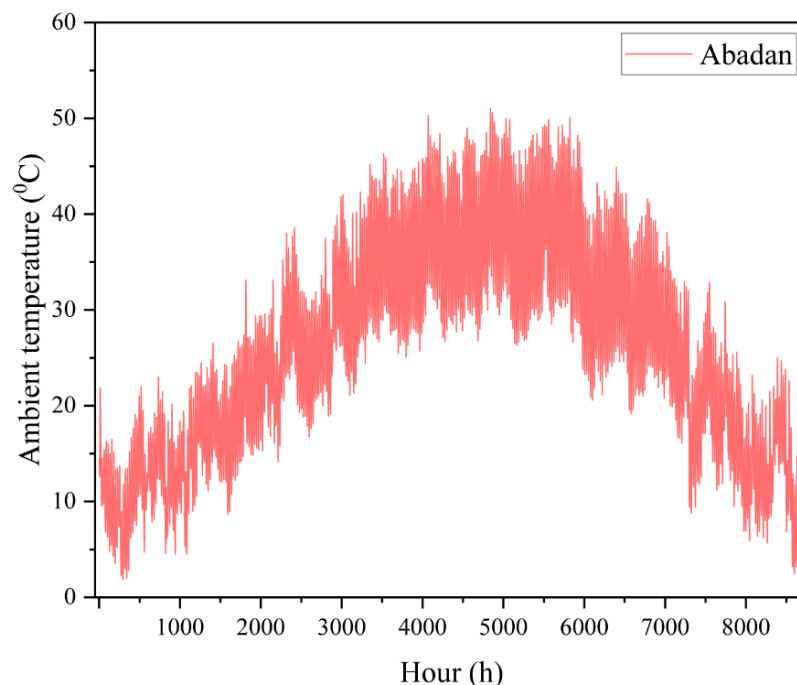


Figure 5. Cont.

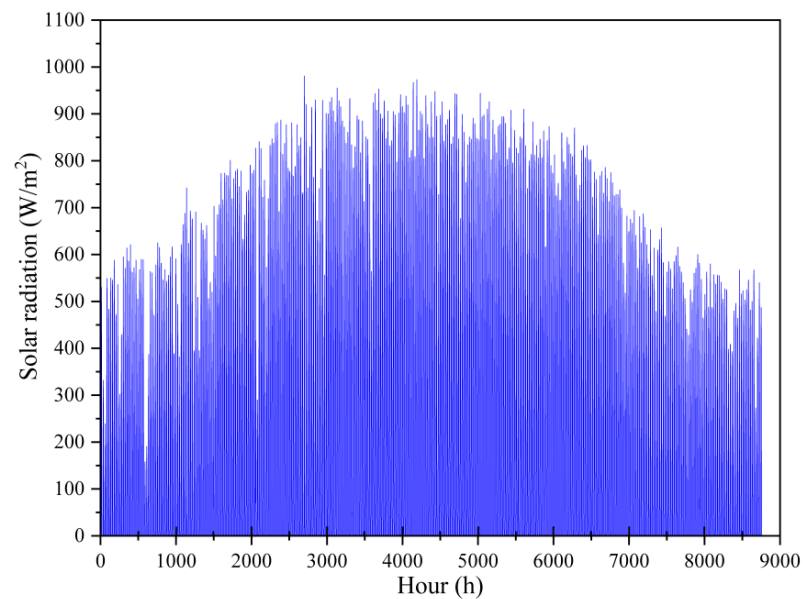


Figure 5. Hourly weather changes in Abadan.

Case Study Results

The effects of both Abadan's air temperature and solar radiation on the solar system during one year are investigated, and the results are depicted in Figure 6. It is apparent that the highest amount of total output work occurs in July and June. Figure 7 shows that the maximum production of freshwater happens during July and June due to the increased sunlight and ambient temperature. Annual energy and freshwater rate production are summarized in Table 8.

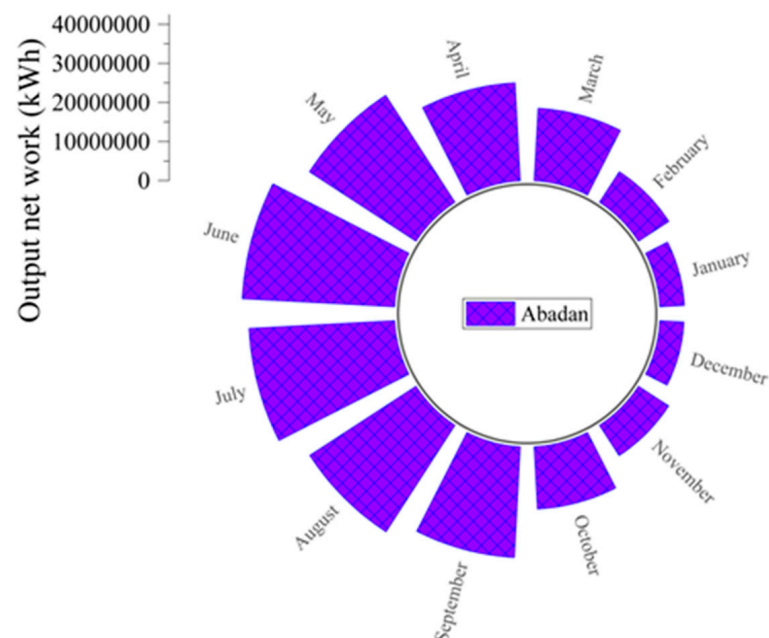


Figure 6. The effect of ambient temperature on the output work during one year.

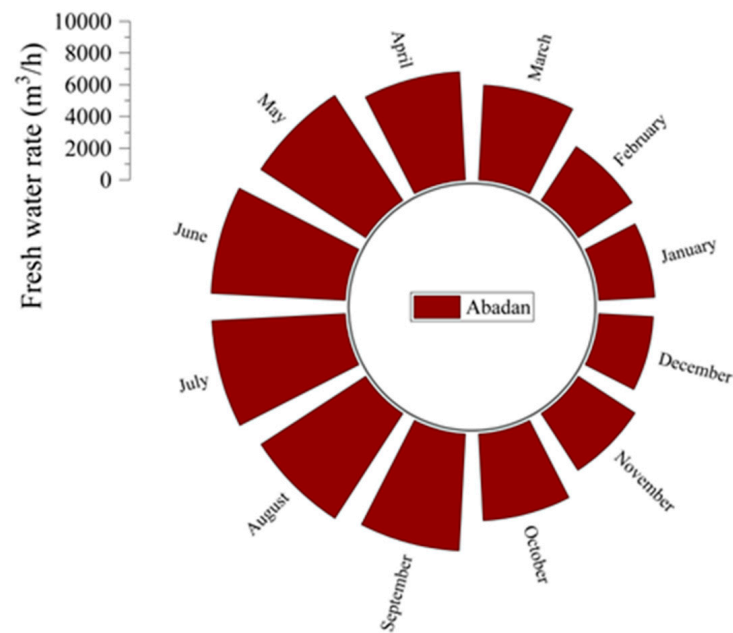


Figure 7. The effect of ambient temperature on the rate of freshwater production during one year.

Table 8. Outputs over a year.

Parameter	Total Power (kW)	Freshwater Water (m ³)
Value	260,847,658.6	73,821.34

5. Optimization Study

5.1. NSGA-II Algorithm

In the multi-objective optimization, the goal is to determine the conditions in which several objective functions are optimized together. In the optimization of thermodynamic problems, there are certain objective functions, which should be minimized or maximized according to the task. In this research, on the basis of the Non-Dominated Sorting Genetic Algorithm II (NSGA-II), maximization of the exergy efficiency and minimization of the cost rate are carried out.

5.2. Optimization Results

In the present study, the optimization of the target functions was performed by increasing excess returns and reducing cost rates. To perform the multi-objective optimization, a code is written to connect the engineering equation solver (EES) with Matlab, which links two platforms in the Dynamic Data Exchange (DDE) method. Table 9 outlines the amount permissible for the design variables used for the optimization.

Table 9. Design variables and their span of changes.

Optimization Variable	Upper Limit	Lower Limit
T ₁ (°C)	400	300
P ₄ (kPa)	1700	1300
Pinch point evaporator (°C)	6	4
Turbine efficiency (%)	0.9	0.7

Figure 8 shows the Pareto efficiency of the solar system. All solution points are determined to be optimal. Furthermore, a simple geometric method is used to select the best point.

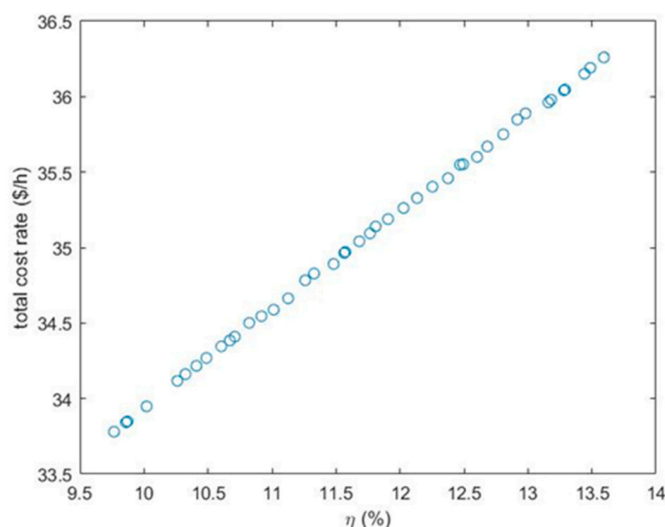


Figure 8. The results of Pareto optimization of the proposed system.

The estimated values of exergy efficiency, cost rate, input temperature to evaporator, input pressure to the turbine, evaporator pinch point and turbine efficiency are summarized in Tables 10 and 11.

Table 10. The optimal result of the objective functions.

Target Function	Value
Exergy efficiency (%)	12.02
Cost (\$/h)	35.26

Table 11. Optimization parameters.

Optimization Parameter	Value
T_1 (°C)	345.05
P_4 (kPa)	1505.22
Evaporator pinch point (°C)	5.62
Turbine efficiency (%)	0.82

6. Conclusions

In this research, the optimization, assessment and modeling of a multi-energy system based on solar power and the utilization of a parabolic trough solar collector were discussed. The products of this energy system included freshwater and electricity. The investigated system consists of parabolic trough solar collector subsystems, a steam Rankine cycle and a reverse osmosis desalination system. Thermodynamic software (EES) is employed to solve the governing equations for the problem and to model the system. Then, according to the results obtained from the system analysis, the best and most effective design parameters of the system's performance, including the turbine efficiency, turbine inlet pressure and solar radiation intensity, were introduced. The city of Abadan was selected as a study case in this research by examining the suitable potential of solar energy. Furthermore, the effects of changes in the ambient temperature of the studied city and variations in the intensity of solar radiation on the work output, freshwater production and exergy efficiency of the system are investigated. In order to optimize the designed system, a version of genetic algorithm (NSGA-II) is considered to determine the value of optimization goals. The Pareto Figure is obtained to determine the best values for the objective functions of the problem, which are the efficiency of the exergy of system and the cost of the system. Finally, the most optimized values of the exergy efficiency and cost rate are calculated to be 12.02% and 35.26 \$/h, respectively.

Author Contributions: Conceptualization, E.A.; Methodology, E.A., N.A. (Nazanin Alaei) and M.L.; Software, E.A. and N.A. (Neha Agarwal); Validation, E.A.; Formal analysis, E.A., M.S. and N.A. (Nazanin Alaei); Investigation, E.A.; Resources, E.A.; Data curation, E.A., N.A. (Neha Agarwal) and N.A. (Nazanin Alaei); Writing—original draft, M.R.A., E.A., M.S. and A.M.; Writing—review & editing, E.A.; Supervision, M.L. All authors have read and agreed to the published version of the manuscript.

Funding: This work was supported by the National Research Foundation of Korea (NRF) grant funded by the Korea government (MSIT) (2021R1A2C1092152).

Data Availability Statement: Not applicable.

Conflicts of Interest: The authors declare no conflict of interest.

Nomenclature

A_{ap}	Aperture area, m ²
A_r	Receiver area, m ²
T	Temperature, °C
P	Pressure, kPa
\dot{Q}	Heat transfer rate, kW
A	Area, m ²
\dot{E}_x	Exergy, kW
F	Feed water mass flow rate, kg/s
C_p	Specific heat of air and water at constant pressure, kJ/kg.K
$C_{p,c}$	Specific heat of working fluid, kJ/kg.K
$D_{o,r}$	Receiver's outside diameter, m
$D_{i,r}$	Receiver's inside diameter, m
G_b	Solar radiation intensity, W/m ²
\dot{m}_c	Mass flow rate in the collector, kg/s
\dot{Q}_u	Collector heat gained, kW
\dot{m}	Mass flow rate, kg/s
S	Absorbed solar radiation, Wm ⁻²
n_{ptc}	Number of collectors
s	Specific entropy, kJ/kg.K
U	Overall heat transfer coefficient, kW/m ² .K
U_L	Heat loss coefficient
h	Specific enthalpy, kJ/kg
h_{fi}	Heat transfer coefficient
x	Salinity, ppm
Z	Investment cost, \$
\dot{Z}	Cost rate, \$/h
FR	Heat removal factor
F1	Collector efficiency factor
K	The ratio of specific heat
W	Power, kW
Subscripts	
PTC	Parabolic trough collector
ORC	Organic Rankine Cycle
RO	Reverse Osmosis

Abbreviations

pp	Pinch point
tur	Turbine
eva	Evaporator
0	Dead state
I	In
e	Out
ph	Physical
ch	Chemical
cv	Control volume
cond	Condenser
sc	Solar collector
Greek symbols	
η	Efficiency
γ	Correction factor for diffuse radiation
τ_C	Transmissivity of the cover glazing, cm^2/s
τ_P	Effective transmissivity of the parabolic trough collector, cm^2/s
α	Absorptivity of receiver

References

- Lopez, J.C.; Escobar, A.; Cárdenas, D.A. Parabolic trough or linear fresnel solar collectors An exergy comparison of a solar-assisted sugarcane cogeneration power plant. *Renew. Energy* **2021**, *165*, 139–150. [[CrossRef](#)]
- Gupta, D.K.; Kumar, R.; Kumar, N. Performance analysis of PTC field based ejector organic Rankine cycle integrated with a triple pressure level vapor absorption system (EORTPAS). *Eng. Sci. Technol. Int. J.* **2020**, *23*, 82–91. [[CrossRef](#)]
- Alirahmi, S.M.; Rahmani, S.; PouriaAhmadi, D.; Wongwises, S. Multi-objective design optimization of a multi-generation energy system based on geothermal and solar energy. *Energy Convers. Manag.* **2020**, *205*, 112426. [[CrossRef](#)]
- Keshavarzadeh, A.H.; Ahmadi, P.; Safaei, M.R. Assessment and optimization of an integrated energy system with electrolysis and fuel cells for electricity, cooling and hydrogen production using various optimization techniques. *Int. J. Hydrogen Energy* **2019**, *44*, 21379–21396. [[CrossRef](#)]
- Qureshy, A.M.M.I.; Dincer, I. Energy and exergy analyses of an integrated renewable energy system for hydrogen production. *Energy* **2020**, *204*, 117945. [[CrossRef](#)]
- Behzadi, A.; Habibollahzade, A.; Ahmadi, P.; Gholamian, E.; Houshfar, E. Multi-objective design optimization of a solar based system for electricity, cooling, and hydrogen production. *Energy* **2019**, *169*, 696–709. [[CrossRef](#)]
- Yüksel, Y.E. Thermodynamic assessment of modified Organic Rankine Cycle integrated with parabolic trough collector for hydrogen production. *Int. J. Hydrogen Energy* **2018**, *43*, 5832–5841. [[CrossRef](#)]
- Gholamian, E.; Habibollahzade, A.; Zare, V. Development and multi-objective optimization of geothermal-based organic Rankine cycle integrated with thermoelectric generator and proton exchange membrane electrolyzer for power and hydrogen production. *Energy Convers. Manag.* **2018**, *174*, 112–125. [[CrossRef](#)]
- Heidarnejad, P.; Genceli, H.; Asker, M.; Khanmohammadi, S. A comprehensive approach for optimizing a biomass assisted geothermal power plant with freshwater production: Techno-economic and environmental evaluation. *Energy Convers. Manag.* **2020**, *226*, 113514. [[CrossRef](#)]
- Ghorbani, B.; BorzooMahyari, K.; Mehrpooya, M.; Hamed, M.H. Introducing a hybrid renewable energy system for production of power and freshwater using parabolic trough solar collectors and LNG cold energy recovery. *Renew. Energy* **2020**, *148*, 1227–1243. [[CrossRef](#)]
- Kianfard, H.; KhalilaryaM, S.; Jafarmadar, S. Exergy and exergoeconomic evaluation of hydrogen and distilled water production via combination of PEM electrolyzer, RO desalination unit and geothermal driven dual fluid ORC. *Energy Convers. Manag.* **2018**, *177*, 339–349. [[CrossRef](#)]
- Alirahmi, S.M.; Assareh, E. Energy, exergy, and exergoeconomics (3E) analysis and multi-objective optimization of a multi-generation energy system for day and night time power generation—Case study: Dezful city. *Int. J. Hydrogen Energy* **2020**, *45*, 31555–31573. [[CrossRef](#)]
- Assareh, E.; Alirahmi, S.M.; Ahmadi, P. A Sustainable model for the integration of solar and geothermal energy boosted with thermoelectric generators (TEGs) for electricity, cooling and desalination purpose. *Geothermics* **2021**, *92*, 102042. [[CrossRef](#)]
- Razmi, A.R.; Janbaz, M. Exergoeconomic assessment with reliability consideration of a green cogeneration system based on compressed air energy storage (CAES). *Energy Convers. Manag.* **2020**, *204*, 112320. [[CrossRef](#)]
- Mehrpooya, M.; Raeesi, M.; Pourfayaz, F.; Delpisheh, M. Investigation of a hybrid solar thermochemical water-splitting hydrogen production cycle and coal-fueled molten carbonate fuel cell power plant. *Sustain. Energy Technol. Assess.* **2021**, *47*, 101458. [[CrossRef](#)]

16. Delpisheh, M.; Haghghi, M.A.; Athari, H.; Mehrpooya, M. Desalinated water and hydrogen generation from seawater via a desalination unit and a low temperature electrolysis using a novel solar-based setup. *Int. J. Hydrogen Energy* **2021**, *46*, 7211–7229. [[CrossRef](#)]
17. Kalogirou, S.A. *Solar Energy Engineering: Processes and Systems*, 2nd ed.; Elsevier: Amsterdam, The Netherlands, 2014.
18. Al-Sulaiman, F.A. Exergy analysis of parabolic trough solar collectors integrated with combined steam and organic Rankine cycles. *Energy Convers. Manag.* **2014**, *77*, 441–449. [[CrossRef](#)]
19. Rashidi, H.; Khorshidi, J. Exergoeconomic analysis and optimization of a solar based multigeneration system using multiobjective differential evolution algorithm. *J. Clean. Prod.* **2018**, *170*, 978–990. [[CrossRef](#)]
20. Nemati, A.; Sadeghi, M.; Yari, M. Exergoeconomic analysis and multi-objective optimization of a marine engine waste heat driven RO desalination system integrated with an organic Rankine cycle using zeotropic working fluid. *Desalination* **2017**, *422*, 113–123. [[CrossRef](#)]
21. Naseri, A.; Bidi, M.; Ahmadi, M.H.; Saidur, R. Exergy analysis of a hydrogen and water production process by a solar-driven transcritical CO₂ power cycle with Stirling engine. *J. Clean. Prod.* **2017**, *158*, 165–181. [[CrossRef](#)]
22. Dincer, I.; Rosen, M.A.; Ahmadi, P. *Optimization of Energy Systems*; John Wiley & Sons, Ltd.: Chichester, UK, 2017.
23. Nafey, A.S.; Sharaf, M.A. Combined solar organic Rankine cycle with reverse osmosis desalination process: Energy, exergy, and cost evaluations. *Renew. Energy* **2010**, *35*, 2571–2580. [[CrossRef](#)]

Disclaimer/Publisher’s Note: The statements, opinions and data contained in all publications are solely those of the individual author(s) and contributor(s) and not of MDPI and/or the editor(s). MDPI and/or the editor(s) disclaim responsibility for any injury to people or property resulting from any ideas, methods, instructions or products referred to in the content.